

Received March 25, 2021, accepted April 25, 2021, date of publication April 28, 2021, date of current version May 5, 2021.

Digital Object Identifier 10.1109/ACCESS.2021.3076219

# Validation of Positive-Sequence Modeling of Large-Disturbance Stability in a Distribution Network With Distributed Generation Using the Hybrid Comprehensive Simulator

ALEKSEY A. SUVOROV<sup>1</sup>, ALISHER B. ASKAROV<sup>1</sup>, MIKHAIL V. ANDREEV<sup>1</sup>,  
AND ALEXANDER S. GUSEV<sup>1</sup>

School of Energy and Power Engineering, Tomsk Polytechnic University, 634050 Tomsk, Russia

Corresponding author: Aleksey A. Suvorov (suvorovaa@tpu.ru)

This work was supported in part by the Russian Science Foundation under the Governmental Grant 18-79-10006, and in part by the Tomsk Polytechnic University Competitiveness Enhancement Program.

**ABSTRACT** One of the general trends in power industry is the penetration of distributed generation (DG) units. The ongoing transformation of electric power systems (EPS) due to this penetration leads to a significant change in the properties of power systems. The problem arises in the ensuring stability of distribution system with DG units and EPS as a whole, especially in the case of large disturbances. The main way of solving this problem is positive-sequence phasor time-domain simulation. However, the known simplifications and limitations are inevitably applied at such simulation. In this regard, the obtained simulation results need to be validated. This paper proposes an alternative approach for validation of processes calculations, based on the use of a benchmark tool instead of field data. The hybrid simulator is proposed to use as a benchmark tool, because such simulator allow to obtain comprehensive information about a single spectrum of wave, electromagnetic, electromechanical processes in power system in cases of different large disturbances. That makes possible to identify the impact of the applied simplifications and limitations in the positive-sequence simulation on the reliability of power system stability assessment in the case of large disturbances. The studies presented in this paper were carried out using the scheme of distribution system with DG units, which is part of a real EPS. The obtained results demonstrate the arising errors in stability calculations, the nature of their changing and causes of occurrence, as well as factors affecting them.

**INDEX TERMS** Cross-validation, power system stability, distributed generation, hybrid simulation, positive-sequence simulation.

## I. INTRODUCTION

Currently, one of the main directions of development and enhancement of electric power systems (EPS) is the penetration of distributed generation (DG) units. It is inevitably lead to a significant mutual impact of transients in the transmission system and distribution network with DG units. Because of this, the control of distribution system with DG units becomes more complicated [1] and, as a consequence, the probability of blackouts increases. In this regard, the assessment and ensuring of distribution system stability seems

The associate editor coordinating the review of this manuscript and approving it for publication was Qiuhua Huang<sup>1</sup>.

to be a non-trivial and relevant challenge, the solution of which becomes even more difficult in the context of DG penetration [2]–[4].

At present, a positive-sequence phasor time-domain simulation is a main approach to study and solve challenges related to the stability of a practical distribution system with DG [5]. However, the total mathematical model of any power system always contains a stiff nonlinear system of differential equations of extremely high order. For improvement in the numerical robustness, a number of simplifications and limitations are applied: (1) decomposition of a single continuous process in EPS, (2) use of single-phase schemes instead of three-phase, (3) simplification of EPS component models,

(4) limitations of the time interval of processes simulation. During modeling conventional power systems, this approach allowed to obtain acceptable results. This is due to the fact that power system stability was determined mainly by high-inertia synchronous generators and their control systems, and it was enough to consider only fairly slow electromechanical phenomena [6]. However, the indicated simplifications can have a significant impact on the reliability of the stability calculations in modern power systems with DG, since in this case the fast transients become determining for power systems dynamics. In this regard, the results of such modeling, currently obtained using various software programs and tools (STs), should be validated [7]. A ‘cross-validation’ of stability calculations for such grids is carried out [8]. A new approach for such validation is presented in this paper. The main feature of the developed approach is used a hybrid multiprocessor simulator as a benchmark tool for obtaining comprehensive information about transients in a distribution systems with DG units. Such approach allows identifying the causes of simulations errors at stability studies by using STs and the affecting factors. The remainder of the paper is organized as follows. Section II is devoted to the analysis of the impact of DG units on the distribution systems stability and factors that determine this impact. Section III describes the proposed approach for the validation of stability calculations. Section IV outlines the principles and approaches to power systems simulation. Section V is devoted to the description of the investigated model of a real power system and the applied validation criteria. Section VI presents the results of experimental studies of the cross-validation procedure. Finally, conclusions are presented in Section VII.

## II. STATE-OF-THE-ART IN THE STABILITY STUDIES OF DISTRIBUTION SYSTEMS WITH DG

At present, a large number of studies have been carried out on the analysis of transients in distributions systems with DG units, the results of which show the impact of DG on all stability types. The DG units improve the damping of electromechanical oscillations, but, at the same time, their frequency increases [1], [9]. The amplitude of power system variables oscillations increases after a disturbance in the EPS, which becomes even greater in the case of DG units’ disconnection from the grid [10]. The amplitude and rate of frequency deviations also increase, on the contrary, the voltage drops become smaller. The indicated impact of DG are associated with their features, the most important of which are a low inertia in compare with conventional generating units and a connection near to the load.

There are various types of DG units with their own characteristics and impact on the stability. The units based on renewable energy sources are predominant, but DG based on low-power synchronous generators (SG-based DG units) connected to the distribution network also has a significant share [11]–[13]. Such units, which include synchronous generator and its excitation system, discussed in this paper.

Quite often, the DG units are connected to the deficient distribution networks that operate as part of the EPS and have weak ties. For such grid, a transition to isolated operation, including after a disturbance, is undesirable, since it inevitably leads to the disconnections of consumers. Therefore, taking into account the need for parallel operation of such distribution systems with the main transmission system during disturbances, there is a significant impact of the external network on transients in the distribution system with DG units and its stability as a whole. In particular, the transmission network elements determine the nature and rate of voltage restoration after a disturbance, which is the main factor determining the stability of distribution system, according to the studies [14]. Due to the complexity of the numerical simulation of large-scale EPSs, in many studies aimed at stability assessment the external network is represented by one equivalent area, thereby completely excluding its impact. However, some authors note the need for a detailed representation of the external network in the analysis of distribution system with DG units stability [15], [16]. Thus, the ongoing changes in the EPS contribute to an increase in the mutual impact of processes in the distribution system and high-voltage transmission network. In this regard, it becomes necessary to model large-scale power systems with a detailed representation of the transmission and distribution networks for the comprehensive stability assessment. It is associated with serious difficulties due to the previously indicated problems of numerical integration. The validation approach presented in this paper allows to assess the impact of applied simplifications and limitations in power system simulation on the reliability of stability calculation of distribution systems with DG units.

Besides to the impact of the transmission systems on transients in distribution networks, the DG units’ features lead to the emergence of new aspects that must be taken into account in distribution systems stability studies. Therefore, the IEEE PES Task Force [17] has developed a new classification of stability, which can be applied to distribution systems with DG units operating in parallel with EPS, due to similar state features and the nature of instability (the authors also note that the current distribution systems are evolving into microgrid). The large disturbances are analyzed for all classes, in contrast to the previously applied approach to assessing microgrid stability, based on linearization techniques and consideration of only small disturbances [18] with obtaining of very limited information [19]. The most critical disturbance is a three-phase-to-ground fault. In this case, significant deviations of power system variables occur and a probability of instability is very high. One of the main and most important indicators determined by fault simulation, especially for distribution systems, is a critical clearing time (CCT), which reflects the stability margin [20]. The calculations validation in the case of faults with a time duration close to a CCT is also important due to the dependence of DG protection on the transients arising during fault [21]. In connection with the above, the current paper provides the results of comprehensive validation of

stability calculations for distribution systems with DG in the case of three-phase faults and an emerging spectrum of processes, especially associated with the operation of DG units' control systems.

From the above analysis, it follows that the stability of distribution systems with DG units has been well studied. However, most of the studies were carried out at a qualitative level, reflecting only the presence of DG impact on transmission system stability or its absence on the example of test small-scale models. This is clearly not enough to carry out a comprehensive and reliable analysis of the stability of modern distribution networks with DG and, accordingly, to develop a reliable control of such grids, in which the penetration level of DG and its impact on the stability continue to increase. In this regard, the cross-validation of stability calculations via STs for distribution systems with DG units as a part of large-scale EPS is an important step towards ensuring the security operation of power systems.

### III. DEVELOPED APPROACH TO VALIDATION

Currently, the main approach to simulation results' validation is its comparison with field data recorded by Phasor Measurement Units [8]. The published results of such validation demonstrate the differences between simulation results and recorded data, which is mainly explained by the discrepancy in the parameters of mathematical model and real EPS [22]–[24]. The adaptation of the calculation results to recorded data used in these studies consists in variations in the models' parameters, mainly in the static characteristics of loads and regulators (or governors). At the same time, it is possible to simulate only main trend of the real process. However, in view of the large number of mathematical models parameters, it is extremely difficult to choose an adequate to the real data set [25]. Also, there are no guarantees that the EPS model adapted with this approach will reliably simulate other states and disturbances that are different from the recorded data used to adapt the EPS model. It is impossible to collect field data for all states and disturbances due to their extreme diversity. In addition, this validation approach does not take into account the simplifications and limitations used in the STs.

Therefore, an important step towards increasing the adequacy and reliability of the simulation results obtained via STs for distribution systems with DG is a cross-validation, which makes it possible to identify the impact of applied simplifications and limitations in positive-sequence STs on the quality of particular processes' simulation and tasks solved with their help. In this paper, the cross-validation is considered in relation to one of the main and most difficult challenges due to its nonlinear nature and rate of processes – ensuring the stability of the distribution systems with DG units, operating in parallel with the external transmission grid in the case of a large disturbance.

The authors of this paper developed an alternative approach based on the use of a comprehensive information obtained via a benchmark tool to carry out the cross-validation of

stability calculations of distribution systems with DG units. Within the framework of the developed approach, an identical mathematical model of EPS is simulated in the considered ST and the benchmark tool. The validation scenarios are being formed. The basis of scenarios is the most critical disturbance, information about which is necessary for reliable and effective stability analysis of distribution network with DG units. The developed validation scenarios are implemented in both the studied ST and the benchmark tool. The obtained simulation results by both tools are compared and analyzed. The benchmark tool should have the properties of sufficiently reliable simulation of a continuous spectrum of quasi steady state and transients on an unlimited time interval in the EPS as a whole. Given the above problems, the numerical simulation tools cannot be applied. Therefore, the authors developed the concept of hybrid power system simulation to create such benchmark tool, which is aggregating and using several modeling approaches (analog, physical and digital) to achieve the indicated properties. The implementation of the hybrid simulation concept is the Hybrid Real-Time Power System Simulator (HRTSim), which has all the above properties and capabilities and can be successfully used as the benchmark tool [26]. An important feature of the developed approach is the possibility of a guaranteed validation of the benchmark tool – HRTSim. The HRTSim validation is possible only according to the data of any state or process of the simulated EPS, e.g. according to the quasi steady state obtained from SCADA. This is possible due to the fact that the same detailed mathematical models of EPS components and a methodologically accurate method for its solution are used in the HRTSim for the entire spectrum of processes. The results of such validation, taking into account the properties and capabilities of the HRTSim, can be extended to the entire significant range of states and processes (0–1000 Hz). The using of the benchmark tool – HRTSim, which can be validate by only one state or process in EPS, instead of the transients' data used in the existing validation methods, is the main novelty of the developed approach.

The reliability of the simulation results obtained via HRTSim is proved by comparison with the field data [27] and widely used hardware and software fully digital multiprocessors simulators like RTDS [28]. The comparisons of the simulation results obtained via the HRTSim and RTDS are carried out just for small schemes. The complexity of reliable numerical integration for small scheme and the problems of large-scale EPS simulation via digital simulators [28] are not manifested. Therefore obtained by digital multiprocessors simulators results can be considered reliable for small schemes and make comparison with them.

### IV. POWER SYSTEM MODELING

The EPS model for large-perturbation stability studies in various STs is presented by following equations system: a system of first-order differential equations (Eq. (1)) describing synchronous and asynchronous machines, their control systems and other EPS components, and a system of

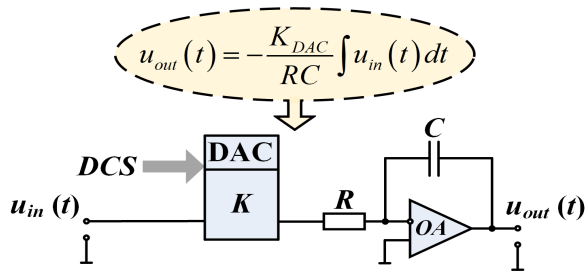


**FIGURE 1.** Description of a continuous implicit integration method: *DCS* is a digital control signal, *DAC* is a digital-to-analog converter, *OA* is an operational amplifier,  $u_{in}(t)$  and  $u_{out}(t)$  are input and output voltages,  $K_{DAC}$  is a gain of DAC.

algebraic equations (Eq. (2)) describing network elements and loads [29].

$$\dot{x} = f(x, y, u) \tag{1}$$

$$0 = g(x, y, u) \tag{2}$$

where  $x$  is a vector of variable conditions of EPS,  $y$  is a vector of parameters,  $u$  is a vector of forcing functions,  $f$  and  $g$  are nonlinear functions.

As opposed to a system of differential-algebraic equations used in all software programs for stability analysis of a large-scale power system, the detailed three-phase mathematical model consisting of stiff nonlinear system of high-order differential equations is used in the HRTSim. A method of continuous implicit integration in analog way is used (Fig. 1) for providing a methodologically accurate, parallel and continuous real-time solution of such system. Also, it allows not to simplify the power systems model, i.e. all transients are described by differential equations including processes of network elements and loads.

The integration operation is implemented via an integrator based on an operational amplifier to eliminate the need for matching and mutual impact of voltage levels of input-output circuits. All information and control functions, e.g. setting the parameters of mathematical models, are digitally implemented via a microprocessor unit (MPU), which consists of several peripheral microprocessors, depending on the type of the modeled EPS element. The interaction of the simulated EPS equipment is carried out at the model physical level ( $u_{max} = 10$  V;  $i_{max} = 5$  mA). A detailed description of this approach, its advantages, and means of its implementation – HRTSim, are presented in Ref. [30].

The electrical machines are the main equipment of any power system and also basis for SG-based DG units considered in this paper. The adequacy and reliability of the calculation results depends on the detailing of the machine mathematical model. Both tools (HRTSim and considered ST) use the same mathematical model of synchronous machine based on the Park equations with a single damper winding on the direct ( $d$ ) and quadrature ( $q$ ) axes (Model 2.1 in Ref. [31]), except excluded in the ST the transformer voltage term. However, the implementation and calculation of this model via a hybrid approach (Fig. 2) differs from the

numerical one. The parameters of the mathematical model are entered into the solution scheme using DACs, as well as the values of excitation voltage  $e_{fd}$ , mechanical  $T_M$  and electromagnetic  $T_E$  torques, which are formed in the MPU as a result of solution of corresponding mathematical models of excitation system, governor and torque equation. The variables  $i_d, i_q$  obtained as a result of the analog solution are entered into the transformation scheme  $d, q \rightarrow A, B, C$ . The coefficients  $K_{id}, K_{iq}$  allow to scale currents and, accordingly, set and change the power of the simulated machine. The mathematical variables of instantaneous values of phase currents, which are continuously formed as a result of this transformation and represented by the voltages  $u \equiv i_A, u \equiv i_B, u \equiv i_C$ , are converted via voltage-current converters (VCC) into the corresponding model physical currents  $i_A, i_B, i_C$ , which are model phase currents of stator windings.

The commutation of the synchronous machines' outputs is implemented via digitally controlled analog switches (DCAS). The instantaneous values of voltages  $u_A, u_B, u_C$ , formed in the output phase nodes of stator windings via voltage followers (VF) and through a transformation scheme  $A, B, C \rightarrow d, q$  are scaled by coefficients  $K_{ud}, K_{uq}$  and entered back into the solution scheme in the form of independent mathematical variables  $u_d, u_q$ . All variables are entered into the analog-to-digital converter processor (PADC) for further processing and visualization.

The processes in the main EPS equipment (electrical machines, transformers, power transmission lines, loads, FACTS devices, etc.) are directly interconnected and the most significant. At the same time, their mathematical models are very conservative and differ mainly in the values of parameters. This gives the reason for their implementation using the approach presented on the example of electrical machine. Accordingly, the specialized hardware-software structures (specialized hybrid processors – SP) of another equipment developed in this way are presented in Ref. [32]. Mathematical models of the main power system components implemented in the HRTSim can be found in Ref. [30]. Auxiliary equipment (control systems, governors, etc.) and its mathematical models are extremely diverse. In this regard, they are simulated in the MPU of each SP.

The separate numerical solution of auxiliary equipment models in different peripheral microprocessors allows to avoid numerical methods problems. The main element of the synchronous machine, which is very sensitive to the occurrence of a large disturbance and determines the nature of transients, is an automatic voltage regulator (AVR) and an excitation system in general. For distribution systems with DG units, the operation of automatic control systems (ACS) has a major impact on the stability in the case of a large disturbance and, as indicated earlier, is included in a separate type of stability. Currently, there are a large number of excitation systems types and their mathematical description. The considered commercial ST has the ability to simulate ACSs, including excitation systems with AVR, of any complexity without simplifications and limitations. In this regard,

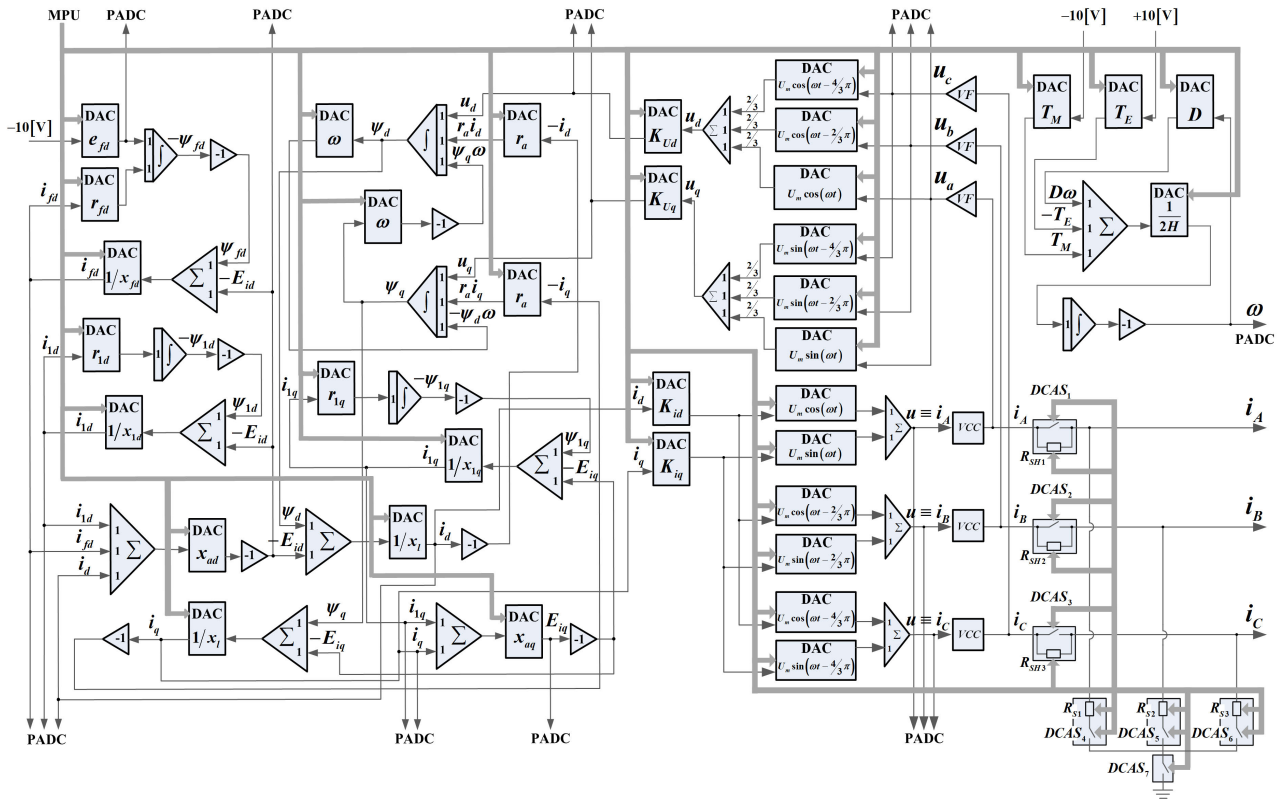


FIGURE 2. Hybrid scheme of synchronous machine simulation.

the current paper discusses identical detailed mathematical models of excitation systems.

**V. POWER SYSTEM DESCRIPTION AND VALIDATION CRITERIA**

**A. MATHEMATICAL MODEL OF THE TEST EPS**

The mathematical model of the large-scale EPS was developed for experimental studies. This model includes a deficient distribution system with SG-based DG units. Static excitation system is modeled with an AVR and a power system stabilizer (PSS). The used model of AVR&PSS based on ST4C with PSS2C. The structure and settings of the AVR and PSS are indicated in each of the experimental cases. The mathematical model GGOV1 recommended by the IEEE for stability studies is used to reproduce the DG units’ governor. The parameters are taken from Ref. [11].

A part of the real power system of Eastern Siberia, Russia, is used as the studied EPS model, a single-line diagram of which is presented in Fig. 3. The model of the test EPS reproduces: the electric network of different voltage level (transmission and distribution networks), taking into account power transmission lines, transformers and loads, as well as the main power plants of this power system (nodes 5–8, 62, 118) and DG units (node 187) with a detailed simulation of each generating unit. Each generating unit simulates its local automatic control system (governor, excitation system, etc.), which corresponds to the actually operated equipment. Thus,

the modeled EPS scheme includes 202 three-phase nodes, 50 electrical machines, 60 power transformers, 114 power transmission lines and 75 static loads (constant impedance load model was used). This model of EPS is reproduced in both the HRTSim and the considered ST for electromechanical transient simulation. Moreover, the mathematical models of auxiliary equipment (control systems, governors, etc.) and their settings implemented in both the ST and the HRTSim are exactly identical. The ST chosen for validation contains sufficiently detailed mathematical models of the power system equipment, a stable numerical integration method, and is a common tool for power system stability analysis. However, despite the high level of the development of this tool, it has all the above-mentioned inevitable simplifications and limitations (see Introduction).

The choice of this EPS is associated with the availability of a sufficiently complete database with necessary information about the parameters and characteristics of EPS equipment (synchronous generators, power transformers, power transmission lines, etc.), including operating algorithms and setting parameters of power system automation, as well as the availability of the validated SCADA data of the simulated EPS. The HRTSim validation was performed by comparing the results of simulating the initial normal operating state of the test EPS with SCADA data. The resulting reproduction match for all nodes and branches is within the SCADA error range of 5%.

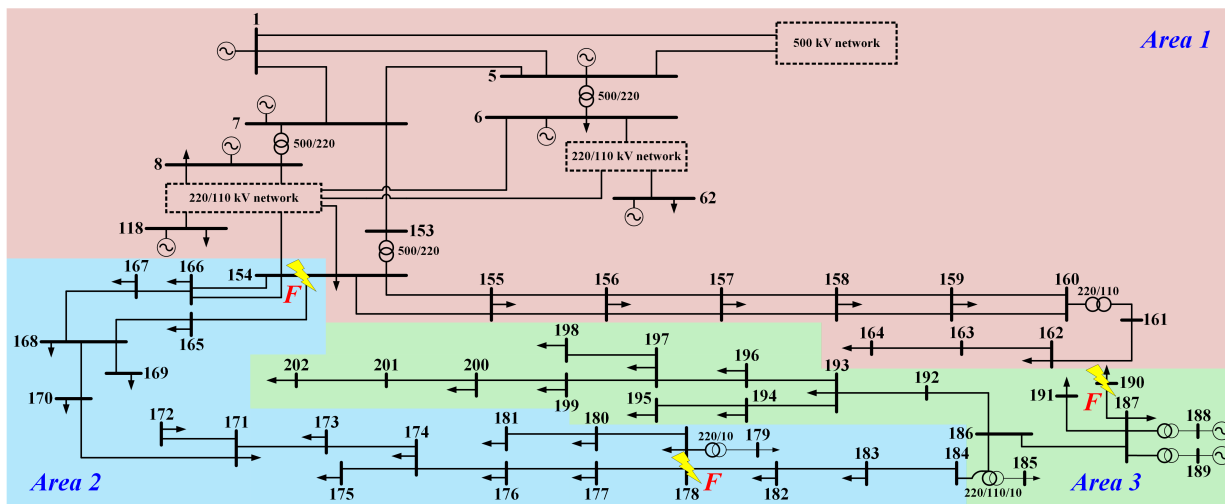


FIGURE 3. Single-line diagram of the test EPS.

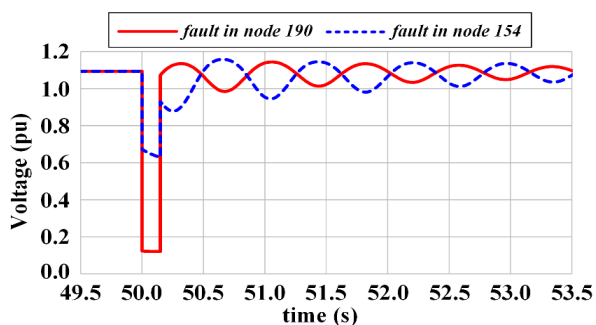


FIGURE 4. Voltage in node 187 in the case of different faults with a time duration of 150 ms.

For a sound planning of disturbance locations, as well as identifying the causes of errors and factors affecting them during experimental studies, the test EPS was analyzed as a two-area power system in which DG units with a small local load (receiving part – Area 3 in Fig. 3) are connected with a bulk power system (sending part – Area 1 in Fig. 3) by a sufficiently long tie line (Area 2 in Fig. 3).

The critical disturbances for DG units located in the receiving part of the EPS are faults at the sending end. During the fault, the transmitted power is dropped, but due to the remoteness of the disturbance, the load of the receiving distribution system decreases slightly, which leads to deceleration of the DG units. At the same time, the stability of DG units is mostly determined by the voltage restoration profile.

After the fault clearing, a sharp increase in the load power at the sending end occurs due to sharp voltage restoration, which leads to a voltage decreasing at the receiving end (Fig. 4, blue dotted line) and can cause an instability in the distribution system. In the case of a fault in the distribution system itself or near the receiving end, the situation is different. During the fault, the DG units are accelerated, because a decrease in the voltage in the receiving part leads to a drop in the load power. After the fault clearing, the power of the

local load at the receiving end increases and the voltage is quickly restored to almost its initial level (Fig. 4, red solid line). In this regard, the boundary points of faults were chosen for the studies: (1) fault in node 154 as a critical disturbance at the bus of the main substation and (2) fault in node 190 as a disturbance close to the DG units.

The process of voltage restoration is determinative for the stability of distribution system with DG units, consequently, the importance of adequate simulation of the network components and external transmission grid in general, which mainly determines this process, is obviously of significant importance.

At the same time, not only detailed modeling of external grid is important, but also the completeness of the network model. Because the completeness of the external grid simulation has a significant impact on the modeling error. To confirm this statement, the network reduction of the test EPS have been implemented via Gauss-reduction method, which is a widespread approach, based on the sequential transformation of a multipath star into an equivalent polygon. Figure 5 shows the equivalent circuit of the test EPS, consisting of 18 three-phase nodes, 8 electrical machines, 7 power transformers, 17 power transmission lines and 12 static loads.

The obtained results (Fig. 6) show that the modeling error disappears due to equivalence of the external grid. The waveforms are different in the full model (green line and violet line at Fig. 6) and they are the similar in the reduced model (red line and blue line at Fig. 6). Thus, there is an error for the full model of test EPS, since the results obtained via ST differ from the benchmark ones obtained via HRTSim. In the equivalent model, there is no error, since the results obtained via ST and HRTSim are the same. That is why the external transmission grid are simulated without reductions in this paper. It allows to identify the impact of the applied simplifications of network elements on the fidelity of stability assessment results.

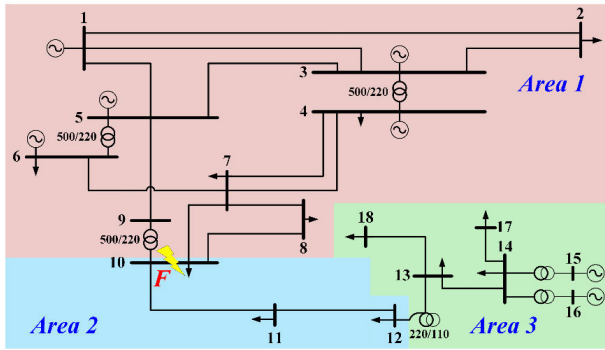


FIGURE 5. Equivalent circuit of the test EPS.

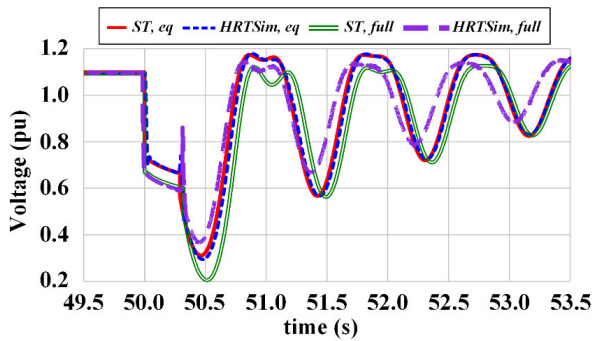


FIGURE 6. Voltage in node 14(187) in the case of fault in node 10(154) with a time duration of 300 ms obtained in equivalent and full model of the test EPS.

**B. VALIDATION CRITERIA**

The validation of calculations of the stability of distribution networks with DG units in the case of a large disturbance can be carried out by qualitative and/or quantitative assessment of modeling results in accordance with a set of certain criteria. The simplest way to perform a qualitative assessment of the model adequacy can be done by visual comparison of the two processes (assessment of the coincidence of oscillation frequencies, their nature of changes and propagation in the power system, assessment of the ACSs’ operation, etc.). However, the use of only qualitative criteria in validation is an insufficient condition for successful cross-validation, the comprehensive implementation of which requires a quantitative assessment of the reliability of the results of numerical modeling and the factors affecting them. The result of the calculation of differential equations in the considered ST is a time-ordered sequence of values, which are time series in general. The results of processes’ simulation in the HRTSim are also time series, since they are a time-ordered set of a sequence of digitized values of model physical variables and the results of numerical integration of ACSs’ mathematical models. In this regard, a quantitative assessment of the reliability of numerical modeling is performed by comparing time series. The frequency and voltage of DG units were chosen as the compared state variables, since their nature mainly determines the stability of distribution system with DG units [17].

TABLE 1. Correlation coefficients.

| Correlation Coefficient ( <i>r</i> ) Value | Interpretation         |
|--|------------------------|
| 0.9 to 1.0                                 | Very high correlation  |
| 0.7 to 0.9                                 | High correlation       |
| 0.5 to 0.7                                 | Moderate correlation   |
| 0.3 to 0.5                                 | Low correlation        |
| 0.1 to 0.3                                 | Negligible correlation |

A comprehensive comparison of time series and, accordingly, a comprehensive cross-validation is performed using various methods aimed at analyzing the single values of elements of both series and the characteristics of the series as a whole at the selected time interval. To assess the reliability of the simulation of the nature and rate of change of the selected parameters, it is proposed to use one of the most common statistical methods for assessing the degree of similarity – correlation analysis, which makes it possible to determine the correlation between the change in the parameters of the power system in the case of disturbances in the ST and HRTSim. To quantify the correlation, the Pearson’s correlation coefficient (*r*) is used [33], the absolute value of which ranges from 0 to 1. The closer *r* is to 1, the more similar the nature of the compared time series is. The correlation coefficient is calculated by Eq. (3), where  $x = (x_1, \dots, x_n)$  is a sample of reference values of the considered parameter (HRTSim data),  $y = (y_1, \dots, y_n)$  is a sample of calculated values of the considered parameter (STs data) and  $\bar{x}, \bar{y}$  are the sample means.

$$r = \frac{\sum_{i=1}^n (x_i - \bar{x}) \cdot (y_i - \bar{y})}{\sqrt{\sum_{i=1}^n (x_i - \bar{x})^2 \cdot \sum_{i=1}^n (y_i - \bar{y})^2}} \tag{3}$$

The calculation of the correlation coefficient is performed for time series with an equal sampling time step. For this purpose, the simulation results obtained via ST and HRTSim were reduced to uniform time stamps using interpolation – nearest-neighbor interpolation method (proximal interpolation). There are several Pearson’s correlation scales which translate the relationship between different variables. This study uses the scale that is shown in Table 1 to identify the relationship between simulation results through the values of Pearson’s correlation coefficient.

At the same time, the scatter plots were used for a graphical comparison of the nature and rate of changes in the EPS parameters. Such diagrams make it possible to identify the form of the dependence obtained between the series (linear or nonlinear). The closer the form is to linear, the better coincidence of the compared series is.

In addition to determining proximity measures between time series based on the values of the elements of time series,

the proximity measure should be assessed based on other characteristics. Moreover, it is necessary that the characteristics are robust in relation to the presence of a trend, changes in the level and scale of the series. Such characteristics are the frequencies of the periodic components of the series. To assess and compare the frequency characteristics of the series, it is proposed to use one of the well-known methods of spectral analysis – the Prony’s method. This method allow to independently assess the amplitudes, frequencies and damping factors of oscillations obtained via ST and HRTSim.

## VI. EXPERIMENTAL RESULTS

Since for the distribution system with DG units, the operation of their ACS is decisive from the point of view of a large-disturbance stability, the experimental studies were carried out in accordance with an approach that assumes a sequential complication of the EPS’ mathematical model by adding ACSs. This approach allows to identify the underlying causes of errors and factors affecting them, as well as the nature of changes in errors during the ACS’ operation. Thus, the experiments are performed for three main cases:

*Case 1:* without operation of ACSs in the test EPS ( $e_{fd} = const$ ,  $T_M = const$ ). The assessment of the error was made that occurs in the simulation results obtained via ST and benchmark tool in the case of a simplification of the EPS’ mathematical model by excluding regulators (and governors) and, accordingly, reducing the stiffness of the system of differential equations forming it (the models of generator controls have time constants several orders of magnitude lower than the other EPS elements).

*Case 2:* with only operation of excitation systems in the test EPS ( $e_{fd} = var$ ,  $T_M = const$ ). The impact of regulators on the level of error was considered, taking into account various AVR algorithms, sets of parameters and structures. The addition of regulators leads to a significant change in the transients during disturbances, which affects the amplitude and nature of the resulting calculation errors.

*Case 3:* with operation of excitation systems and governors in the test EPS ( $e_{fd} = var$ ,  $T_M = var$ ). The results for this case are not presented, since the resulting nature of the error is similar to Case 2.

### A. VALIDATION RESULTS IN THE CASE OF $E_{FD} = CONST$ AND $T_M = CONST$

**Case 1.1.** To assess the impact of the network component on the calculation error, which occurs due to the algebraic calculation of network elements in the ST, the faults with different location and time duration were considered: close and far distance faults with a time duration of  $0.5t_{CCT}$ ,  $0.9t_{CCT}$ , and  $t_{CCT}$ . In the course of experimental studies, it was revealed that in the case of a close fault (node 190), the error is practically absent in the results obtained via ST (Figs. 7 and 8). The results obtained using the ST and the HRTSim practically coincide, the correlation coefficients for voltage and frequency are greater than 0.9, which indicates a very high degree of reliability of the ST simulation results for

close faults of any duration. This is due to the fact that with such a disturbance, the resulting transients mainly depend on the response of electrical machines, which in the ST are reproduced with high reliability, despite the neglecting of transformation electromotive forces in the model of the electrical machine. The impact of the network component is minimal. In addition, the values of a CCT are the same (see Subsection C).

For graphical display of the form of dependence between the simulation results obtained via ST and HRTSim, the corresponding scatter plots are shown in Figs. 7–10. The highlighted region in the scatter plot of voltages (Fig. 7(b)) characterizes the switching moments (occurrence and clearing of fault), forming a ‘gap’ between the values. This is due to the algebraic calculation of the network in the considered ST, in which an instantaneous voltage change occurs. An increase in the time duration for close fault up to  $t_{CCT}$  does not lead to an error (with an increase from  $0.5t_{CCT}$  to  $t_{CCT}$ , the correlation coefficient for frequency decreased by 2.5% from 0.9858 to 0.9610). When the fault location is removed from the DG units (node 178) towards the main substation, there is no significant change in the error level due to the weak impact of the network elements on transients in the considered distribution system. The correlation coefficients obtained for the faults in nodes 190 and 178 of different time durations are greater than 0.9, which indicates a very high degree of reliability of the simulation results according to Table 1 for such disturbances.

The largest differences were obtained for the far distance and critical disturbance – fault at the bus of the main substation (node 154). When the time duration of fault is  $0.5t_{CCT}$  the error is minimal, but as the time duration of the fault increases up to  $t_{CCT}$ , the error level also increases. The correlation coefficient at  $t_{CCT}$  was 0.3673, which shows a low degree of reliability of the simulation results obtained via ST. Such change in error level is associated with an increase in the intensity of transients in the network, and its algebraic reproduction instead of differential leads to differences in the amplitudes of oscillations, the level of their damping, etc. (Figs. 9 and 10). Moreover, the greatest error occurs after the fault clearing, when the voltage is restored (Fig. 9), which strongly depends on the transients in the external transmission system. The different nature of the voltage in the node with DG units leads to different transients in the electrical machines themselves, as evidenced by the frequency oscillogram and its scatter plot (Fig. 10). The obtained scatter plots (Figs. 9(b) and 10(b)) have a pronounced nonlinear character, reflecting significant differences in the obtained simulation results. In addition, a significant increase in the calculation error clearly demonstrates the trend in the change in the correlation coefficients for different locations of faults, which is presented in Table 2.

The resulting histogram of the total error, which is reflected by the Pearson’s correlation coefficient, in the case of faults with different location and time duration is shown in Fig. 11. Figure 11 and the following histograms show the values of

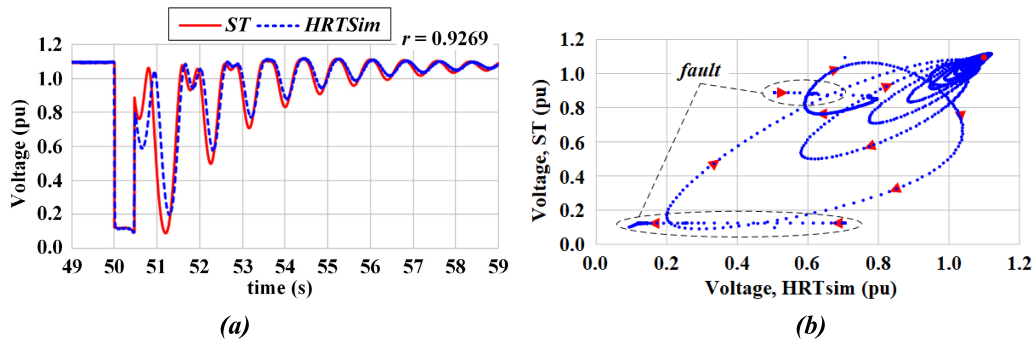


FIGURE 7. Voltage in node 187 (a) and corresponding scatter plot (b) in the case of a fault in node 190 with a time duration of  $t_{CCT}$ .

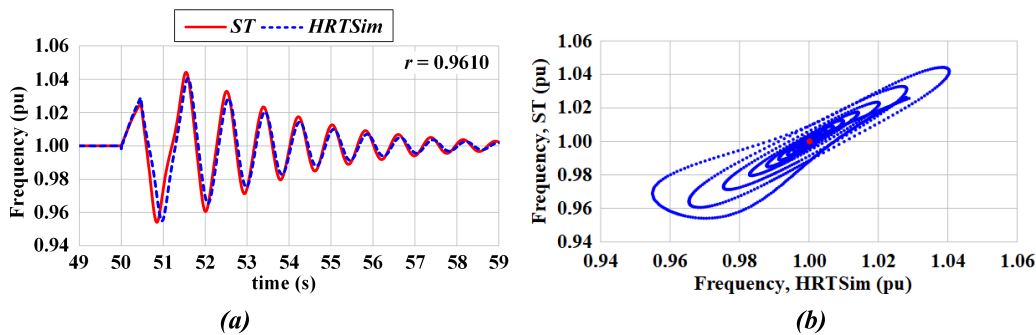


FIGURE 8. Frequency of DG units (a) and corresponding scatter plot (b) in the case of a fault in node 190 with a time duration of  $t_{CCT}$ .

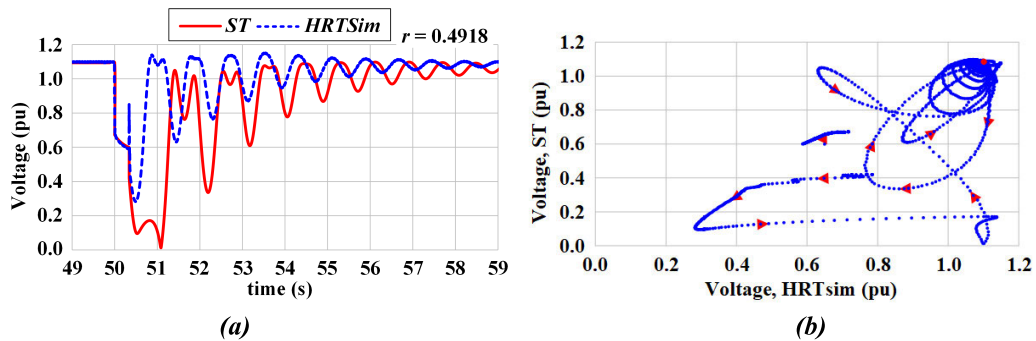


FIGURE 9. Voltage in node 187 (a) and corresponding scatter plot (b) in the case of a fault in node 154 with a time duration of  $t_{CCT}$ .

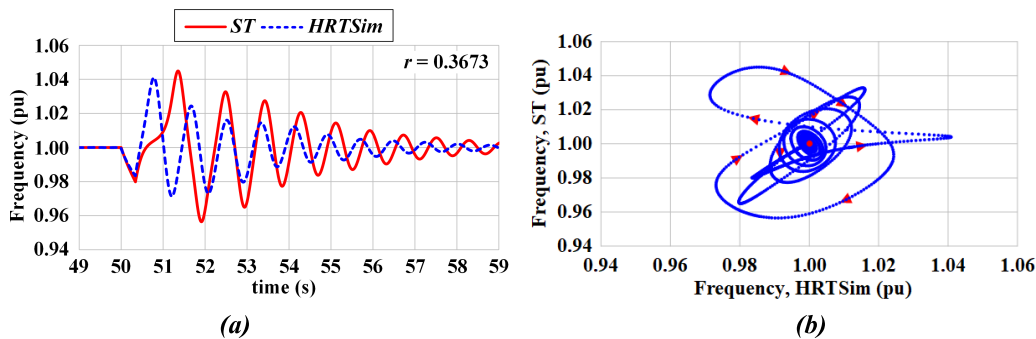


FIGURE 10. Frequency of DG units (a) and corresponding scatter plot (b) in the case of a fault in node 154 with a time duration of  $t_{CCT}$ .

the correlation coefficients for the frequency, the correlation coefficients for the voltage and other operating parameters follow similar patterns. In connection with the obtained

results, the assessment of simulation level error in case of the critical disturbance (fault at the bus of the main substation in node 154) is described further in this paper.

TABLE 2. Summary table of correlation coefficients for case 1.1.

| Case 1.1                            | Correlation Coefficient ( $r$ ) |              |
|-------------------------------------|---------------------------------|--------------|
|                                     | for $U_{187}$                   | for $f_{DG}$ |
| close fault (Figs. 7 and 8)         | 0.9269                          | 0.9610       |
| far distance fault (Figs. 9 and 10) | 0.4918                          | 0.3673       |

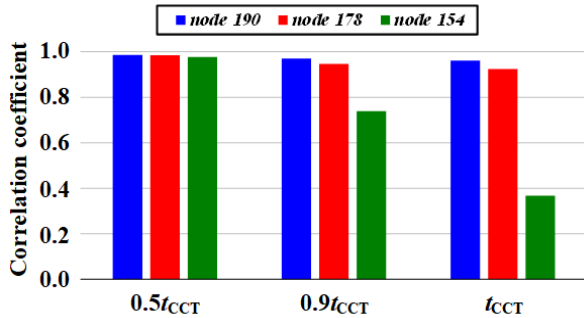


FIGURE 11. Correlation coefficients for the frequency of DG units in the case of faults with different location and time duration.

TABLE 3. Inertia constant and windings time constants for DG units.

| Parameter      | DG Type |         |
|----------------|---------|---------|
|                | $DG(1)$ | $DG(2)$ |
| $H$ (MW·s/MVA) | 3.340   | 1.209   |
| $T_{jd}$ (s)   | 1.556   | 0.286   |
| $T_{ld}$ (s)   | 0.091   | 0.019   |
| $T_{lq}$ (s)   | 0.106   | 0.028   |

**Case 1.2.** As indicated in Section II, various SG-based DG units are currently being used. Moreover, for such units, not only the ACSs differ, but also the SGs themselves. Since SG largely determines the nature of transients, the analysis of the impact of SG parameters on the resulting calculation error has been carried out. For this purpose, in addition to the SG with the basic set of parameters ( $DG(1)$ ) considered in all experimental cases, another SG ( $DG(2)$ ) with lower values of the inertia constant and windings time constants of an electrical machine (Table 3) is used.  $DG(2)$  is typical for modern power systems, processes in which become faster. A full list of the SGs' parameters is given in Appendix A.

In this case, it was experimentally revealed that the use of SGs with significantly lower values of time constants leads to an increase in the error in the simulation results (Fig. 12). The correlation coefficients for the fault with a time duration of  $t_{CCT}$  were 0.3673 for  $DG(1)$  and 0.1792 for  $DG(2)$ , i.e. the change in the parameters led to an increase in the total error by 51%.

An increase in the error level is associated with a significant change in the nature of transients during disturbance

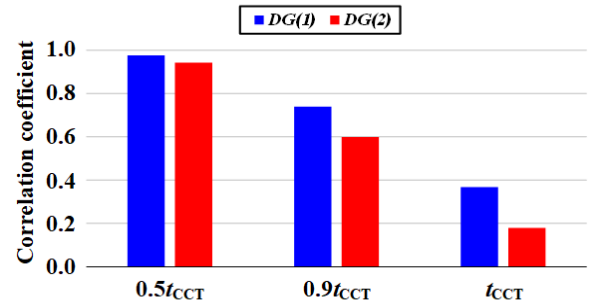


FIGURE 12. Correlation coefficients for the frequency of DG units with different parameters in the case of faults in node 154 with different time duration.

(Fig. 13). The SG with the second set of parameters ( $DG(2)$ ) has lower values of inertia and winding time constants, which leads to a significant increase in the amplitude of oscillations after fault clearing. Significant deviations at the beginning of the transients are the major cause of the emergence of large differences throughout the entire process of oscillation damping. Even despite the fact that in this case the damping of post-fault oscillations increases (the damping factor in the HRTSim is 0.44 for  $DG(1)$  and 1.08 for  $DG(2)$ ). In addition, the use of DG units with  $DG(2)$  parameters leads to an increase in the error in determining the CCT compared to  $DG(1)$  (see Subsection C).

**Case 1.3.** For distribution system with DG units, a characteristic feature is the increased value of the  $R/X$  ratio in comparison with the transmission network due to the larger number of cable power transmission lines [17]. An increase in this ratio improves the stability of distribution system in the case of large disturbances [14]. Taking into account the significant role of the  $R/X$  ratio, the analysis of its impact on the calculation error has been carried out.

An increase in the  $R/X$  ratio by 30% relative to the initial value in the studied distribution system leads to a decrease in the level of calculation error. The correlation coefficient increased to 0.5147, which indicates a moderate degree of reliability of the simulation results obtained via ST, even in the case of a fault with a time duration of  $t_{CCT}$ . When the  $R/X$  ratio decreases, the opposite situation is observed, the correlation coefficient becomes 0.2202, which already corresponds to a negligible degree of reliability of the simulation results (Table 1). The histogram with the correlation coefficients is shown in Fig. 14.

Changes in the error for this case are associated with the impact of the network component. Since the equation of network elements in general differential form (Eq. (4)) has a characteristic equation (Eq. (5)), it follows that the parameter  $L$  (the same as  $X = \omega L$ ) determines the degree of impact of the differential component on the calculation results.

$$L \frac{di}{dt} + Ri = u \tag{4}$$

$$Lp + R = 0 \tag{5}$$

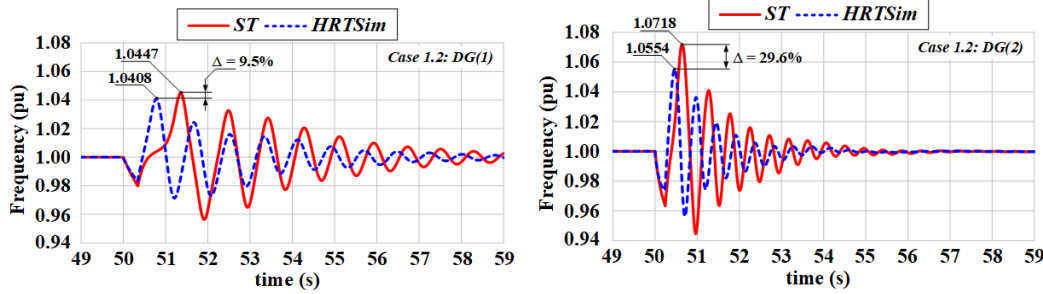


FIGURE 13. Frequency of DG units with different parameters in the case of a fault in node 154 with a time duration of  $t_{CCT}$ .

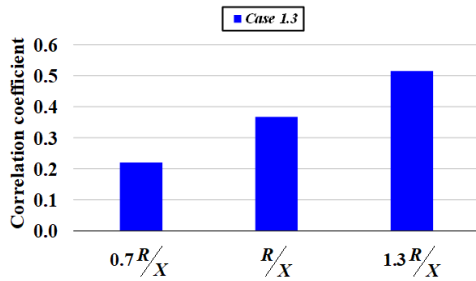


FIGURE 14. Correlation coefficients for the frequency of DG units with different  $R/X$  ratio in the case of a fault in node 154 with a time duration of  $t_{CCT}$ .

With increasing  $R/X$  ratio (in the limiting case, it can be obtained  $u = Ri$ ), the impact of different representations of network elements decreases, which affects the decrease in the error level, and vice versa. Thus, in distribution systems with a predominance of cable power transmission lines and a large value of resistance in general, the modeling error will be less, even in the case of a fault with a time duration close to or equal to a CCT.

**Case 1.4.** The change of DG' penetration level from 15% to 140% was considered to assess its impact on the error in stability calculations in the case of large disturbances. The DG penetration level ( $PL$ ) in the test EPS is calculated by Eq. (6), where  $P_{DG}$  is the total DG units' power generation and  $P_{Load}$  is the total load demand.

$$PL(\%) = \frac{\Sigma P_{DG}}{\Sigma P_{Load}} \cdot 100\% \quad (6)$$

According to the obtained results, the error changes insignificantly with an increase in the penetration level in the case of a fault with  $0.5t_{CCT}$  at the bus of the main substation. The lowest value of the correlation coefficient equal to 0.8106 was obtained for the case of  $PL = 120\%$ , which generally indicates a high/very high degree of reliability of the simulation results obtained via ST for such disturbances (Fig. 15).

With an increase in the time duration of fault up to a CCT, the resulting error begins to change depending on the penetration level. As the total DG units' power generation increases, the error decreases until the total load demand

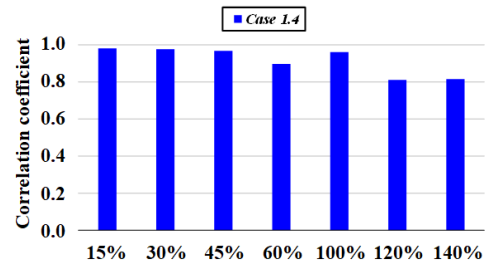


FIGURE 15. Correlation coefficients for the frequency of DG units with different penetration level in the case of a fault in node 154 with a time duration of  $0.5t_{CCT}$ .

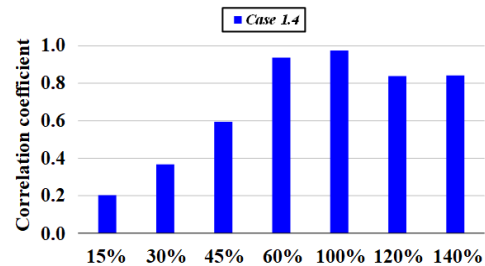


FIGURE 16. Correlation coefficients for the frequency of DG units with different penetration level in the case of a fault in node 154 with a time duration of  $t_{CCT}$ .

and power generation are equalized ( $P_{DG} = P_{Load}$ ) for the studied distribution system (the correlation coefficient increased from 0.2032 to 0.9748). After that, the value of the correlation coefficient is in the range from 0.8 to 0.9 (Fig. 16).

An increase in the DG' penetration level changes the structure of the test EPS, which leads to a change in the direction of power flows and, consequently, lower voltage drops during disturbances, a higher rate of its restoration, as well as a lower degree of intensity of transients in general (amplitude of oscillations, their damping) (Fig. 17). As a result, the dependence of transients in the distribution system on the external network elements decreases, which leads to a decrease in the error due to the different reproduction of the network component, even in the case of a fault with a time duration of  $t_{CCT}$ .

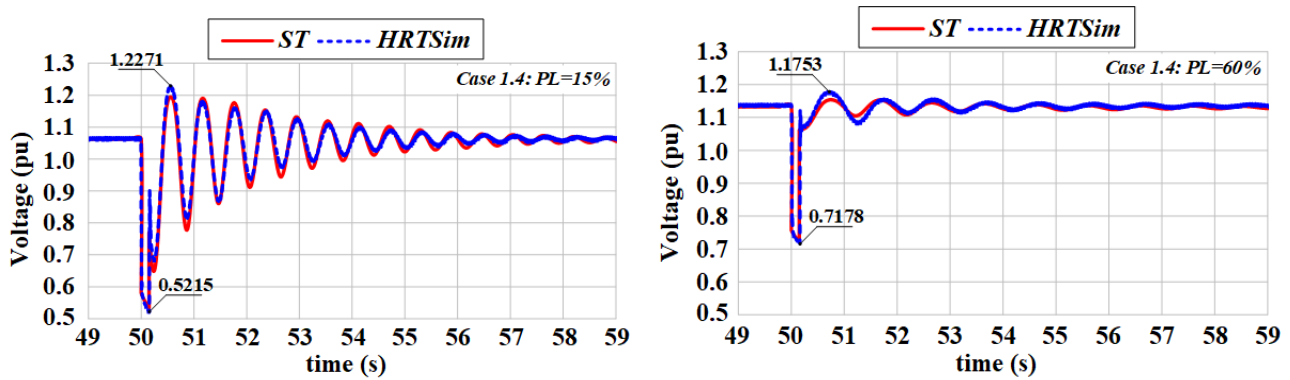


FIGURE 17. Voltage in node 187 with different DG penetration level in the case of a fault in node 154 with a time duration of 150 ms.

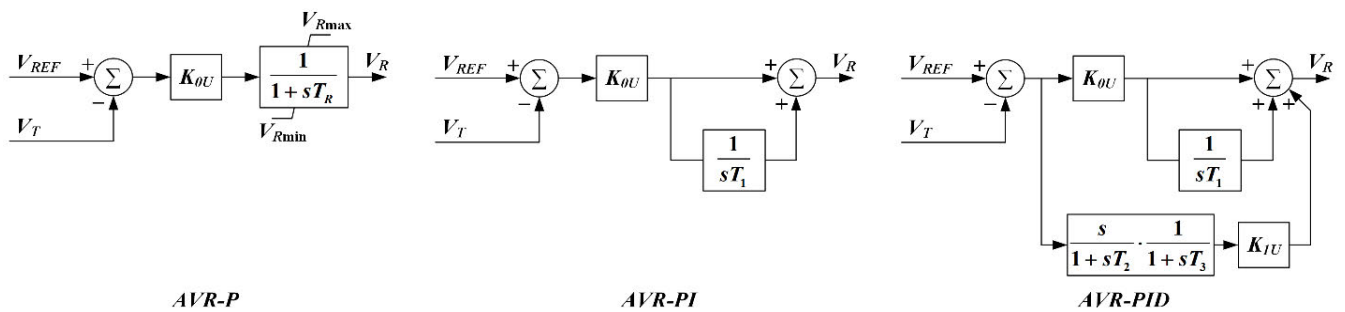


FIGURE 18. Structures of AVR models.

TABLE 4. AVR settings.

| AVR type | Data set | $K_{OU}$ (pu) | $T_I$ (s) | $K_{IU}$ (pu) |
|----------|----------|---------------|-----------|---------------|
| AVR-P    | 1        | 10.0          | -         | -             |
|          | 2        | 50.0          | -         | -             |
| AVR-PI   | 1        | 3.0           | 2.0       | -             |
|          | 2        | 15.0          | 2.0       | -             |
| AVR-PID  | 1        | 3.0           | 2.0       | 2.0           |
|          | 2        | 3.0           | 2.0       | 10.0          |

**B. VALIDATION RESULTS IN THE CASE OF  $E_{FD} = VAR$  AND  $T_M = CONST$**

**Case 2.1.** Since the main ACS of SG-based DG units responding to a large disturbance and determining stability is AVR, the analysis of the impact of AVR operation on the resulting calculation error has been carried out in the case of different AVR algorithms and settings. For this purpose, the basic algorithms are considered: proportional (P), proportional-integral (PI) and proportional-integral-differential (PID) with various gains (Fig. 18 and Table 4). These algorithms are the most common and are used in most excitation systems (DC1C, AC1C, ST8C, etc.).

The simulation of AVR leads to an increase in the error level (Fig. 19), which is due to its response and an increase in

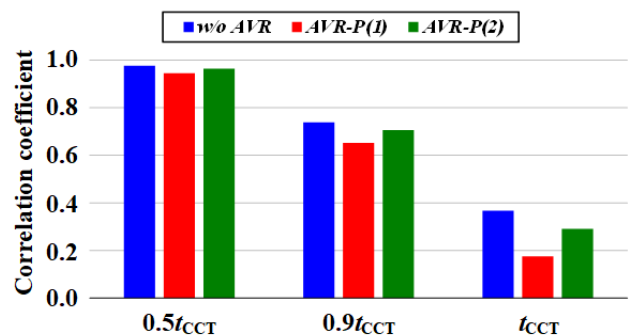


FIGURE 19. Correlation coefficients for the frequency of DG units with AVR - P operation in the case of faults in node 154 with different time duration.

the primary differences in voltage at the terminals of DG units that occur at the initial stage of the transients. The correlation coefficient decreased by 12% (from 0.7390 to 0.6515) in the case of a fault with a time duration of  $0.9t_{CCT}$  without AVR and with AVR - P(1) and by 52% (from 0.3673 to 0.1749) in the case of a fault with  $t_{CCT}$ .

At the same time, improving the damping of post-fault oscillations by setting large gains for the AVR channels (e.g., AVR - P(2)) leads to a decrease in the error in obtained results, including fault with  $t_{CCT}$  (Fig. 20). Despite this, the error is still at a significant level – the correlation coefficient for

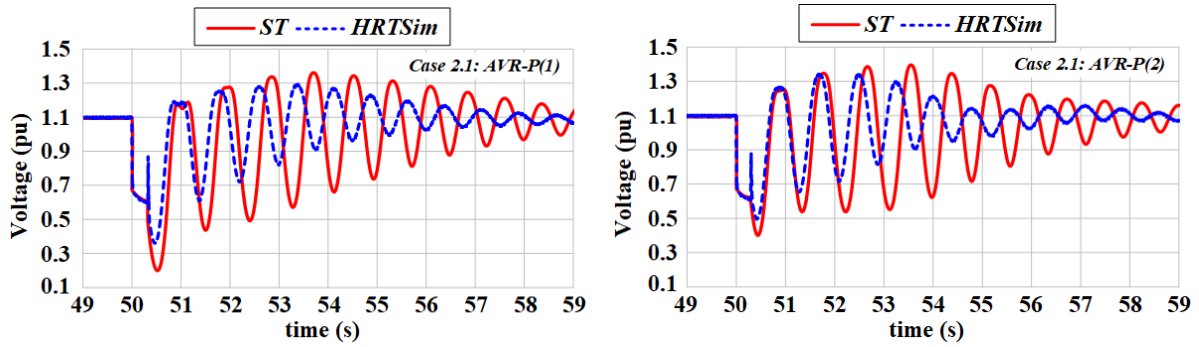


FIGURE 20. Voltage in node 187 with different AVR – P settings in the case of a fault in node 154 with a time duration of  $t_{CCT}$ .

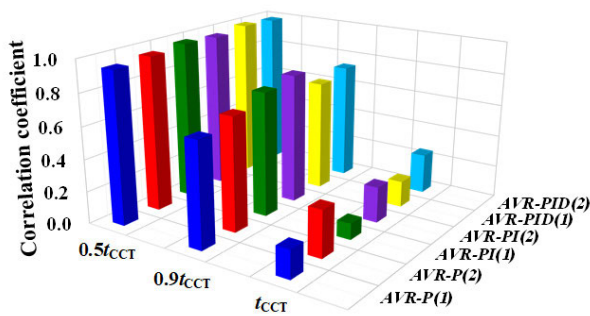


FIGURE 21. Correlation coefficients for the frequency of DG units with AVR operation in the case of faults in node 154 with different time duration.

AVR – P(1) is equal to 0.1749 in the case of a fault with  $t_{CCT}$ , for AVR – P(2) – 0.2910. As a result, the gains changing led to a decrease in the error level by 66%.

Changes in the AVR algorithm insignificantly affect the nature of the error change (Fig. 21). With short-time duration faults, the error is still practically absent. As the time duration of the disturbance increases up to  $t_{CCT}$ , the error also increases. Thus, when considering critical faults with a time duration close to  $t_{CCT}$ , the values of the correlation coefficients do not exceed 0.3, which indicates a negligible degree of reliability of the simulation results obtained via ST.

The lowest correlation coefficient for the fault with  $t_{CCT}$ , equal to 0.1003, was obtained with the operation of AVR – PI(1), the highest  $r$ , equal to 0.2910, – for AVR – P(2). Taking into account AVR operation with different algorithms and settings does not increase the differences in a CCT (see Subsection C).

**Case 2.2.** To assess the impact of the PSS on the nature of the resulting error, stabilizing channels with different input parameters (the rotor current  $i_f$  for AVR&PSS1 and the generator voltage frequency  $f_u$  for AVR&PSS2) and settings were added to the AVR – PID structure (Fig. 22 and Table 5) [34].

The consideration of a PSS leads to an additional increase in the error compared to the case of AVR only operation (Fig. 23). The PSS also amplifies the primary differences. However, the AVR operation continues to have a significant

impact on the error value, which is associated with its more intense response to a significant error in the nature of voltage restoration at the initial moment of fault clearing due to the algebraic calculation of network elements. The introduction of only rotor current channels (AVR&PSS1) leads to an insignificant increase in the error by ~5% relative to the AVR only operation. The introduction of voltage frequency channels (AVR&PSS2) has a greater impact on the error value in the simulation results obtained via considered ST.

In the case of a fault with a time duration of  $t_{CCT}$  without AVR and with AVR&PSS2(1) operation, the correlation coefficient decreased by 62% (from 0.3673 to 0.1406) (Fig. 23), for the case of AVR – PID(1), the decrease was 52%. The major cause of this is the dependence of the ACS' operation on several operating parameters ( $u$ ,  $i_f$  and  $f_u$ ) and its response not only to the deviation of the absolute values of the controlled parameters, but also to the rate of their change. The impact of the PSS settings on the nature of the error is shown in Fig. 24.

An increase in the gains for AVR&PSS1 leads to a slight increase in the error by ~6% (from 0.1581 to 0.1473). In the case of AVR&PSS2 operation with different settings, the error changes more significantly. To identify the causes of such changes, a spectral analysis of the resulting oscillations in the frequency of DG units was carried out by the Prony method. The results are shown in Table 6, the oscillograms of frequency are shown in Fig. 25. The amplitude ( $A$ ), frequency ( $f$ ) and damping factor ( $\alpha$ ) of the dominant mode were determined by used Prony method. The error values ( $\Delta$ ) were calculated relative to the HRTSim. The obtained differences in the frequency of oscillations ( $f$ ) are insignificant and are within 3%. The values of the amplitude and damping factor vary significantly.

For the case of AVR&PSS2(1), the error in the amplitude of the dominant mode is about 80%, which is directly related to a significant difference in the damping factor ( $\Delta\alpha = 46\%$ ). The gains' increasing (AVR&PSS2(2)) leads to a deterioration in the damping of post-fault oscillations by 31% (according to the HRTSim' results the damping factor for AVR&PSS2(1) is 0.5178, for AVR&PSS2(2) – 0.3571), but at the same time this reduces the error in amplitude and damping factor

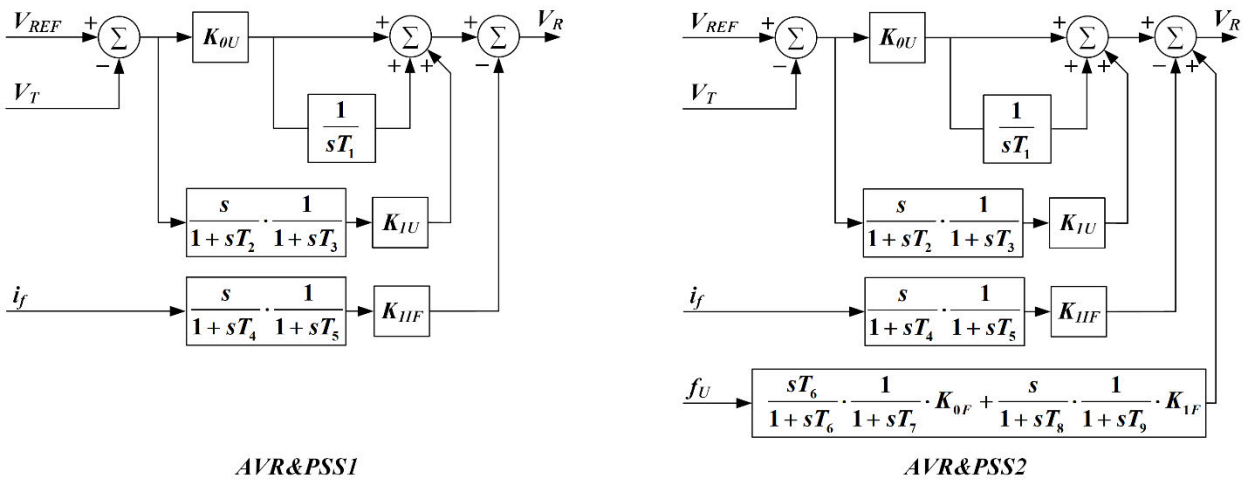


FIGURE 22. Structures of AVR&PSS models.

TABLE 5. AVR&PSS settings.

| AVR type | Data set | $K_{OU}$ (pu) | $T_I$ (s) | $K_{IU}$ (pu) | $K_{IF}$ (pu) | $K_{OF}$ (pu) | $K_{IF}$ (pu) |
|----------|----------|---------------|-----------|---------------|---------------|---------------|---------------|
| AVR&PSS1 | 1        | 3.0           | 2.0       | 2.0           | 1.8           | -             | -             |
|          | 2        | 3.0           | 2.0       | 2.0           | 3.0           | -             | -             |
| AVR&PSS2 | 1        | 3.0           | 2.0       | 2.0           | 1.8           | 2.0           | 1.25          |
|          | 2        | 3.0           | 2.0       | 2.0           | 1.8           | 4.0           | 5.0           |

TABLE 6. Prony analysis results.

| Case        | ST     |        |                | HRTSim |        |                | $\Delta A$ (%) | $\Delta f$ (%) | $\Delta \alpha$ (%) |
|-------------|--------|--------|----------------|--------|--------|----------------|----------------|----------------|---------------------|
|             | A (pu) | f (Hz) | $\alpha$ (1/s) | A (pu) | f (Hz) | $\alpha$ (1/s) |                |                |                     |
| AVR&PSS2(1) | 0.0128 | 1.3617 | 0.2773         | 0.0071 | 1.3951 | 0.5178         | 80.28          | 2.40           | 46.45               |
| AVR&PSS2(2) | 0.0131 | 1.3333 | 0.2242         | 0.0084 | 1.3625 | 0.3571         | 55.95          | 2.14           | 37.22               |

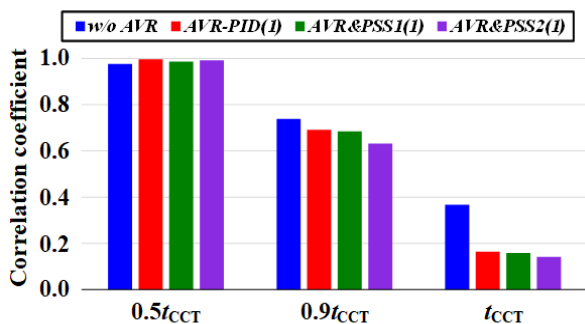


FIGURE 23. Correlation coefficients for the frequency of DG units with AVR&PSS operation in the case of faults in node 154 with different time duration.

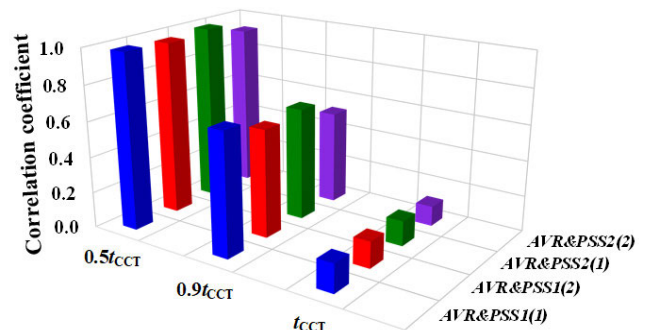


FIGURE 24. Correlation coefficients for the frequency of DG units with AVR&PSS operation in the case of faults in node 154 with different time duration and different PSS' settings.

of the dominant mode. Despite this, the resulting error at AVR&PSS2(2) increases by 20% for the case of fault with  $t_{CCT}$ . The correlation coefficient decreased from 0.1406 for

AVR&PSS2(1) to 0.1122 for AVR&PSS2(2). The increase in the error is due to a much more intense response of a PSS to differences in the amplitude of the dominant mode.

TABLE 7. Differences in the CCT obtained via ST and benchmark tool.

| Case     | Model       | $t_{CCT}$ (ms) |        |                  |          |        |                  |
|----------|-------------|----------------|--------|------------------|----------|--------|------------------|
|          |             | Node 190       |        |                  | Node 154 |        |                  |
|          |             | ST             | HRTSim | $\Delta t_{CCT}$ | ST       | HRTSim | $\Delta t_{CCT}$ |
| Case 1.2 | DG(1)       | 490            | 490    | 0                | 340      | 360    | 20               |
|          | DG(2)       | 290            | 280    | -10              | 240      | 310    | 70               |
| Case 2.1 | AVR-P(1)    | 400            | 410    | 10               | 320      | 350    | 30               |
|          | AVR-P(2)    | 370            | 370    | 0                | 290      | 320    | 30               |
|          | AVR-PI(1)   | 390            | 390    | 0                | 310      | 340    | 30               |
|          | AVR-PI(2)   | 380            | 370    | -10              | 310      | 340    | 30               |
|          | AVR-PID(1)  | 460            | 450    | -10              | 310      | 350    | 40               |
|          | AVR-PID(2)  | 470            | 470    | 0                | 310      | 340    | 30               |
| Case 2.2 | AVR&PSS1(1) | 460            | 450    | -10              | 320      | 360    | 40               |
|          | AVR&PSS1(2) | 480            | 470    | -10              | 330      | 370    | 40               |
|          | AVR&PSS2(1) | 480            | 470    | -10              | 330      | 380    | 50               |
|          | AVR&PSS2(2) | 470            | 480    | 10               | 370      | 420    | 50               |

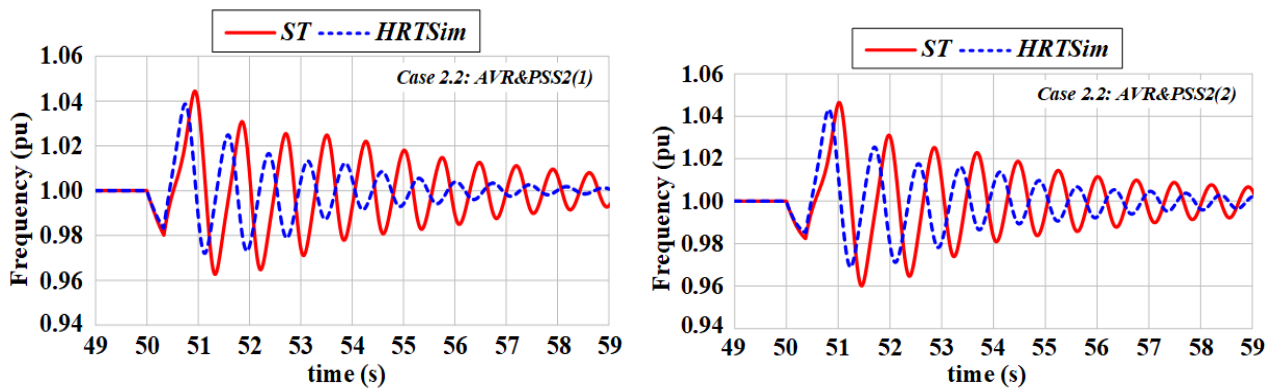


FIGURE 25. Structures of AVR&PSS models.

According to the Bode plot of the considered structure of AVR&PSS2 (Fig. 26), a change in the setting leads to an amplification in the signal of the dominant mode frequency by more than 4 times.

Summarizing the above, the complication of the AVR mathematical model by adding stabilizing channels deteriorates the reliability of the simulation results obtained via ST. In addition, taking into account a PSS causes an increase in the differences in a CCT obtained via ST and benchmark tool (see Subsection C).

C. ERROR IN CCT CALCULATIONS

Taking into account the high significance of the CCT' value, an assessment of the differences in its calculations for the cases of a close and far distance fault using the benchmark tool and ST was made. The results are shown in the summary Table 7. The greatest differences occur only for the

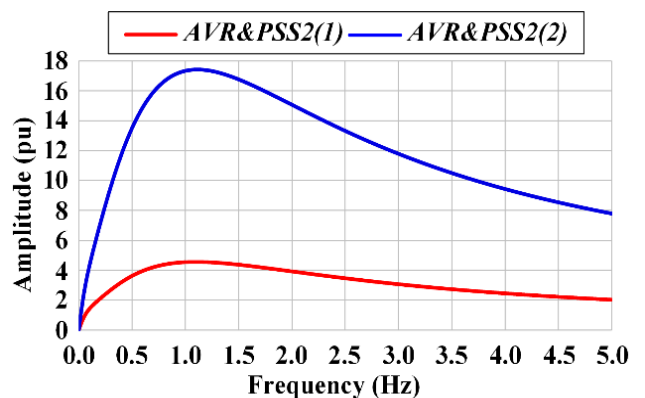


FIGURE 26. Bode plot of AVR&PSS2(1) and AVR&PSS2(2).

cases of a far distance fault (in the HRTSim,  $t_{CCT}$  is always greater by 30–70 ms), for a close fault they are insignificant

TABLE 8. Parameters of SG.

| Parameter      | DG Type |        |
|----------------|---------|--------|
|                | DG(1)   | DG(2)  |
| $r_a$ (pu)     | 0.0006  | 0.0053 |
| $x_l$ (pu)     | 0.1440  | 0.1700 |
| $x_d$ (pu)     | 0.8700  | 2.0450 |
| $x'_d$ (pu)    | 0.2700  | 0.2460 |
| $x''_d$ (pu)   | 0.2030  | 0.1510 |
| $x_q$ (pu)     | 0.5400  | 2.0450 |
| $x''_q$ (pu)   | 0.2280  | 0.2160 |
| $T'_{d0}$ (s)  | 8.6800  | 4.5894 |
| $T''_{d0}$ (s) | 0.2000  | 0.0979 |
| $T''_{q0}$ (s) | 0.5000  | 0.6097 |

(within 10 ms). Differences in the CCT are directly related to the level of error in the simulation results. Moreover, the greater error at the initial stage of transients, the more the difference will be in the value of a CCT obtained via ST and benchmark tool. For example, when changing the parameters of SG in the Case 1.2, it is shown that the use of DG(2) leads to an increase in the error in the simulation results (the correlation coefficient for the fault with  $t_{CCT}$  decreased from 0.3673 to 0.1792). At the same time, the obtained value of a CCT in ST is more different ( $\Delta = 70$  ms) from the similar value obtained in the HRTSim than in the case of using DG(1) ( $\Delta = 20$  ms). The change in the parameters of SG led to an increase in the differences in a CCT by 50 ms. The operation of AVRs with different algorithms in the Case 2.1 does not lead to significant differences in a CCT (it is approximately at the level of 30 ms). The addition of a PSS causes an additional increase in the error in the simulation results for the considered ST, which leads in turn to large differences in the values of a CCT (it is already at the level of 40–50 ms for Case 2.2).

## VII. CONCLUSION

The increasing level of DG penetration changes the nature of transients and the properties of power systems. Taking into account the significant mutual impact of processes in the transmission systems and the distribution networks with DG units, it is necessary to consider a large-scale mathematical model of EPS without significant equivalence for a reliable solution of the stability challenges. At present, various STs based on a positive-sequence phasor time-domain simulation are used for this purpose. With such modeling, a number of known simplifications and limitations are applied, which in the study of conventional power systems did not significantly affect the comprehensiveness and reliability of the results obtained. However, this is not always the case for distribution networks with DG units. In this regard, a relevant task to improve the reliability of the simulation results is the implementation of validation.

The validation approach proposed in this paper consists in use information from the benchmark tool – the HRTSim and eliminates the need to have a huge number of field data for its implementation. It should be emphasized that the approach was developed taking into account the further use of STs for the calculation of the stability of distribution systems with DG units. The STs have obvious practical advantages over the HRTSim, which cannot replace them. The HRTSim described in this paper is a complex software and hardware simulator, the industrial production and large-scale application of which is a very expensive and time-consuming process, the implementation of which can currently be considered as some long-term prospect. At the same time, the developed experimental prototype can be used as a benchmark tool due to its properties and capabilities. In this regard, the proposed approach to validation makes it possible to assess the reliability of the obtained results in the case of various disturbances with different intensity and location.

The cross-validation performed using the developed approach allows to identify the causes of calculation errors and the factors affecting them, as well as to identify disturbances and emerging processes calculated with the greatest error. The simulation results of such processes require further more detailed analysis before their using in practical challenges. Due to this, the level of reliability in the results of a positive-sequence modeling increases, since it becomes possible to know exactly in which cases there will be an error, as well as its value and reasons.

This paper demonstrates the most critical cases with an error. The experimental studies have shown that the greatest error in calculating the stability of distribution system in the case of a large disturbance occurs at a fault in a critical point, in particular at the bus of the main substation, when the impact of the network component on transients is the greatest. A error is due to a simplification of the calculation of network elements. However, when a distribution system with DG units becomes independent from the external network in terms of transmitted power the resulting error decreases. In addition, an increase in the R/X ratio also has a positive impact on the error. For all other possible faults, the simulation results in a positive-sequence modeling showed a very high degree of reliability. In addition, in these cases, there was no error in CCT calculation.

A decrease in the inertia of SG for DG units leads to an increase in the calculation error. The use of ACS in the EPS' mathematical model leads to a change of the level of error. The AVR operation has the main impact, regardless of its structure, since it directly responses to differences in the nature of the voltage at the initial stage of transients. The addition of a PSS has a similar impact on the error. However, in this case, with an increase in the number of controlled parameters, the error also increases. This is due to the fact that a PSS additionally responses to the resulting error in each of the parameters. Further research will focus on

the cross-validation of stability calculations of power system with converter-interfaced generators.

## APPENDIX A

See Table 8

## REFERENCES

- [1] N. Gaeini, A. M. Amani, M. Jalili, and X. Yu, "Cooperative secondary frequency control of distributed generation: The role of data communication network topology," *Int. J. Electr. Power Energy Syst.*, vol. 92, pp. 221–229, Nov. 2017.
- [2] E. Nasr-Azadani, C. A. Canizares, D. E. Olivares, and K. Bhattacharya, "Stability analysis of unbalanced distribution systems with synchronous machine and DFIG based distributed generators," *IEEE Trans. Smart Grid*, vol. 5, no. 5, pp. 2326–2338, Sep. 2014.
- [3] M. Pertl, T. Weckesser, M. Rezkalla, and M. Marinelli, "Transient stability improvement: A review and comparison of conventional and renewable-based techniques for preventive and emergency control," *Electr. Eng.*, vol. 100, no. 3, pp. 1701–1718, Sep. 2018.
- [4] E. P. Madruga, D. P. Bernardon, R. P. Vieira, and L. L. Pfitscher, "Analysis of transient stability in distribution systems with distributed generation," *Int. J. Electr. Power Energy Syst.*, vol. 99, pp. 555–565, Jul. 2018.
- [5] I. Xyngi, A. Ishchenko, M. Popov, and L. van der Sluis, "Transient stability analysis of a distribution network with distributed generators," *IEEE Trans. Power Syst.*, vol. 24, no. 2, pp. 1102–1104, May 2009.
- [6] P. Kundur, P. Kundur, J. Paserba, V. Ajjarapu, G. Andersson, A. Bose, C. Canizares, N. Hatziaargyriou, D. Hill, A. Stankovic, C. Taylor, and T. Van Cutsem, "Definition and classification of power system stability IEEE/CIGRE joint task force on stability terms and definitions," *IEEE Trans. Power Syst.*, vol. 19, no. 3, pp. 1387–1401, May 2004.
- [7] H. Guo, C. Zheng, H. H.-C. Iu, and T. Fernando, "A critical review of cascading failure analysis and modeling of power system," *Renew. Sustain. Energy Rev.*, vol. 80, pp. 9–22, Dec. 2017.
- [8] J. Bialek, E. Ciapponi, D. Cirio, E. Cotilla-Sanchez, C. Dent, I. Dobson, P. Henneaux, P. Hines, J. Jardim, S. Miller, M. Panteli, M. Papic, A. Pitto, J. Quiros-Tortos, and D. Wu, "Benchmarking and validation of cascading failure analysis tools," *IEEE Trans. Power Syst.*, vol. 31, no. 6, pp. 4887–4900, Nov. 2016.
- [9] K. Sundaramoorthy, V. Thomas, T. O'Donnell, and S. Ashok, "Virtual synchronous machine-controlled grid-connected power electronic converter as a ROCOF control device for power system applications," *Electr. Eng.*, vol. 101, no. 3, pp. 983–993, Sep. 2019.
- [10] A. M. Azmy and I. Erlich, "Impact of distributed generation on the stability of electrical power system," in *Proc. IEEE Power Eng. Soc. Gen. Meeting*, San Francisco, CA, USA, Jun. 2005, pp. 1056–1063.
- [11] P. Pourbeik, "Dynamic models for turbine-governors in power system studies," IEEE Task Force Turbine-Governor Model., NJ, USA, Tech. Rep. PER-TR1, 2013, p. 117.
- [12] S. Granville, P. Lino, F. Ralston, L. A. Barroso, and M. Pereira, "Recent advances of sugarcane biomass cogeneration in Brazil," in *Proc. IEEE Power Energy Soc. Gen. Meeting*, Calgary, AB, Canada, Jul. 2009, pp. 1–5.
- [13] M. Wang and J. Zhong, "Development of distributed generation in China," in *Proc. IEEE Power Energy Soc. Gen. Meeting*, Calgary, AB, Canada, Jul. 2009, pp. 1–7.
- [14] A. Ishchenko, "Dynamics and stability of distribution networks with dispersed generation," Ph.D. dissertation, Technische Universiteit Eindhoven, Eindhoven, The Netherlands, 2008, p. 182, doi: [10.6100/IR632007](https://doi.org/10.6100/IR632007).
- [15] J. C. Boemer, M. Gibescu, and W. L. Kling, "Dynamic models for transient stability analysis of transmission and distribution systems with distributed generation: An overview," in *Proc. IEEE Bucharest PowerTech*, Bucharest, Romania, Jun./Jul. 2009, pp. 1–8.
- [16] P. Panciatici, G. Bareux, and L. Wehenkel, "Operating in the fog: Security management under uncertainty," *IEEE Power Energy Mag.*, vol. 10, no. 5, pp. 40–49, Sep. 2012.
- [17] M. Farrokhbadi et al., "Microgrid stability definitions, analysis, and examples," *IEEE Trans. Power Syst.*, vol. 35, no. 1, pp. 13–29, Jan. 2020.
- [18] R. Majumder, "Some aspects of stability in microgrids," *IEEE Trans. Power Syst.*, vol. 28, no. 3, pp. 3243–3252, Aug. 2013.
- [19] J. Sun, "Small-signal methods for AC distributed power systems—A review," *IEEE Trans. Power Electron.*, vol. 24, no. 11, pp. 2545–2554, Nov. 2009.
- [20] M. Pavella, D. Ernst, and D. Ruiz-Vega, *Transient Stability of Power Systems: A Unified Approach to Assessment and Control*. New York, NY, USA: Springer, 2000.
- [21] *IEEE Standard for Interconnection and Interoperability of Distributed Energy Resources with Associated Electric Power Systems Interfaces*, IEEE Std 1547-2018, Apr. 2018, p. 138.
- [22] R. Villena-Ruiz, A. Honrubia-Escribano, J. Fortmann, and E. Gómez-Lázaro, "Field validation of a standard type 3 wind turbine model implemented in DIGSILENT-PowerFactory following IEC 61400-27-1 guidelines," *Int. J. Electr. Power Energy Syst.*, vol. 116, Mar. 2020, Art. no. 105553.
- [23] *Pan European Grid Advanced Simulation and State Estimation*. Accessed: Jan. 13, 2021. [Online]. Available: <https://cordis.europa.eu/project/id/211407>
- [24] P. Overholt, D. Kosterev, J. Eto, S. Yang, and B. Lesieutre, "Improving reliability through better models: Using synchrophasor data to validate power plant models," *IEEE Power Energy Mag.*, vol. 12, no. 3, pp. 44–51, May 2014.
- [25] Z. Huang, T. B. Nguyen, D. Kosterev, and R. Guttromson, "Model validation of power system components using hybrid dynamic simulation," in *Proc. IEEE/PES Trans. Distr. Conf. Exhib.*, Dallas, TX, USA, May 2006, pp. 153–160.
- [26] A. Suvorov, A. Gusev, M. Andreev, and A. Askarov, "The novel approach for electric power system simulation tools validation," *Electr. Eng.*, vol. 101, no. 2, pp. 457–466, Jun. 2019.
- [27] A. Suvorov, A. Gusev, M. Andreev, and A. Askarov, "A validation approach for short-circuit currents calculation in large-scale power systems," *Int. Trans. Electr. Energy Syst.*, vol. 30, no. 4, pp. 1–20, Apr. 2020.
- [28] A. Suvorov, A. Gusev, N. Ruban, M. Andreev, A. Askarov, R. Ufa, I. Razzhivin, A. Kievets, and J. Bay, "Potential application of HRTSim for comprehensive simulation of large-scale power systems with distributed generation," *Int. J. Emerg. Electr. Power Syst.*, vol. 20, no. 5, pp. 1–13, Oct. 2019.
- [29] P. Kundur, *Power System Stability and Control*. New York, NY, USA: McGraw-Hill, 1994, p. 1199.
- [30] A. A. Suvorov, A. A. Z. Diab, A. S. Gusev, M. V. Andreev, N. Y. Ruban, A. B. Askarov, R. A. Ufa, I. A. Razzhivin, A. V. Kievets, Y. D. Bay, V. E. Rudnik, R. Aboelsaud, A. Ibrahim, and A. S. Al-Sumaiti, "Comprehensive validation of transient stability calculations in electric power systems and hardware-software tool for its implementation," *IEEE Access*, vol. 8, pp. 136071–136091, 2020.
- [31] *IEEE Recommended Practice for Excitation System Models for Power System Stability Studies*, IEEE Std 421.5-2016, Aug. 2016, p. 207.
- [32] M. Andreev, I. Razzhivin, A. Suvorov, N. Ruban, R. Ufa, A. Gusev, Y. Bay, A. Kievets, A. Askarov, and V. Rudnik, "A hybrid model of type-4 wind turbine—Concept and implementation for power system simulation," in *Proc. IEEE PES Innov. Smart Grid Technol. Eur. (ISGT-Europe)*, The Hague, The Netherlands, Oct. 2020, pp. 799–803.
- [33] K. Sareen, B. R. Bhalja, S. Srivastava, Y. Swarnkar, and R. P. Maheshwari, "Islanding detection technique based on Karl Pearson's coefficient of correlation for distribution network with high penetration of distributed generations," *Int. J. Emerg. Electr. Power Syst.*, vol. 19, no. 3, 2018, Art. no. e20170232.
- [34] A. L. Komkov, E. N. Popov, N. Y. Filimonov, A. A. Yurganov, and A. A. Burmistrov, "Implementing the system functions of the automatic proportional-derivative excitation control of synchronous generators," *Power Technol. Eng.*, vol. 53, no. 3, pp. 356–359, Sep. 2019.



**ALEKSEY A. SUVOROV** received the Engineering and Ph.D. degrees from National Research Tomsk Polytechnic University, Russia, in 2014 and 2018, respectively. He is currently an Associate Professor with the Division for Power and Electrical Engineering, School of Energy and Power Engineering, National Research Tomsk Polytechnic University. His research interests include transient processes simulation and power systems stability issues.

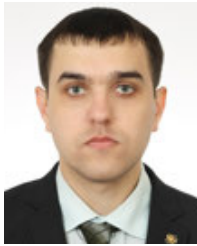


**ALISHER B. ASKAROV** received the M.Sc. degree from National Research Tomsk Polytechnic University, Russia, in 2018, where he is currently pursuing the Ph.D. degree with the Division for Power and Electrical Engineering, School of Energy and Power Engineering. He is currently a Research Engineer with the Research and Development Laboratory for Electrical Power Systems Simulation. His research interests include simulation of automation control systems and renewables.



**ALEXANDER S. GUSEV** received the D.Sc. (Tech.) degree in electrical engineering from Tomsk Polytechnic University, Tomsk, Russia, in 2008. He is currently a Professor with the Division for Power and Electrical Engineering, Tomsk Polytechnic University. His research interest includes simulation of large-scale EPSs.

...



**MIKHAIL V. ANDREEV** received the Engineering and Ph.D. degrees from National Research Tomsk Polytechnic University, Russia, in 2010 and 2013, respectively. He is currently the Head of the Research and Development Laboratory for Electrical Power System Simulation and an Associate Professor with the Division for Power and Electrical Engineering, School of Energy and Power Engineering, National Research Tomsk Polytechnic University. His research interests include simulation of relay protection and automation control systems.